Assessing selected natural and anthropogenic impacts on freshwater lens morphology on small barrier Islands: Dog Island and St. George Island, Florida, USA

James C. Schneider · Sarah E. Kruse

Abstract The freshwater lens morphologies of the barrier islands Dog Island and St. George Island on the panhandle coast of Florida (FL), USA, are controlled to varying degrees by both natural and anthropogenic factors. Variable-density groundwater flow models confirm that spatial variability of recharge values can account for the observed lens asymmetry on these islands. The depth to the base of the lens does not vary significantly seasonally. Human development has altered recharge patterns in some areas, locally thinning the freshwater lens. Aqueduct water supply to St. George Island represents ~7–25% of natural recharge; higher recharge rates are required to simulate the lens on St. George Island than on Dog Island. On both islands, coastal erosion rates are sufficiently rapid that the freshwater lens may not be in equilibrium with current boundary conditions.

Résumé La morphologie des lentilles d'eau douce des îles de Dog et de St. George, situés dans le district côtier de Florida-Etats Unis est contrôlé dans une mesure variable par des facteurs naturelles et humaines. Les modèles d'écoulement à densité variable des eaux souterraines confirment que la variation spatiale de la recharge peut expliquer les asymétries observées des lentilles des cettes îles. La profondeur des lentilles ne présente pas des variations saisonnières importantes. Les activités humaines ont modifié la recharge dans certaines zones en amincissant localement les lentilles d'eau douce. L'alimentation en eaux de l'île de St. George représente 7–25% de la recharge naturelle; pour simuler les lentilles de l'île de Dog il a été nécessaire d'introduire des valeurs plus élevées de la recharge par rapport aux ceux utilisés pour l'île de St. George. Pour les deux îles l'érosion côtière est assez rapide ainsi que les lentilles de eau douce ne sont pas en équilibre avec les conditions à la frontière.

Received: 2 October 2003 / Accepted: 3 January 2005
Published online: 9 April 2005

J. C. Schneider (✉) · S. E. Kruse
Department of Geology, University of South Florida,
4202 East Fowler Ave. Tampa, FL, 33620 USA
e-mail: jschnei4@chuma.cas.usf.edu
e-mail: skruse@cas.usf.edu

Resumen Las morfologías de los lentes de agua dulce en las islas de barrera: Islas Dog y St. George, en la costa alargada y estrecha de Florida, EUA, están controladas en diferentes grados por factores antropogénicos y naturales. Los modelos de flujo con densidad variable del agua subterránea, confirman que la variabilidad espacial de los valores de recarga, pueden ser la causa de la asimetría observada en los lentes de estas islas. La profundidad hasta la base de los lentes no varía significativamente con las estaciones climáticas. El desarrollo humano ha alterado las tendencias de recarga en algunas áreas, causando adelgazamiento local de los lentes de agua dulce. El abastecimiento de agua del acueducto en la Isla St. George, representa entre 7% y 25% de la recarga natural; por otro lado se necesitan cantidades mayores de recarga para simular los lentes en la Isla St. George que en la Isla Dog. En ambas islas, las tasas de erosión costera son tan rápidas, que las lentes de agua dulce podrían no estar en equilibrio con las condiciones actuales de frontera.

Keywords Salt-water/fresh-water relations · Numerical modeling · Water supply · Coastal aquifers · Coastal erosion

Introduction

The long-term "equilibrium" morphology (size and shape) of the freshwater lens on small islands is controlled by many factors, including island stratigraphy, elevation and vegetation patterns, and unequal sea level and tidal effects (e.g., Wheatcraft and Buddemeier 1981; Urish and Ozbilgin 1989; Vacher and Quinn 1997; Collins and Easley 1999; Schneider and Kruse 2003). These factors in turn affect aquifer parameters (i.e., horizontal and vertical hydraulic conductivity) and boundary conditions (i.e., recharge and saltwater head), which determine the development of the freshwater lens. Superimposed on and interrelated with the longer-term "stable" controls on lens form are transient processes such as seasonal variability (precipitation and evaporation), changes in island area (accretion and erosion), and anthropogenic factors, such as pumping and alteration of vegetation and elevation.

The islands considered here, St. George Island and Dog Island, FL (Fig. 1), are intriguing sites for hydrogeologic

 DOI 10.1007/s10040-005-0442-9

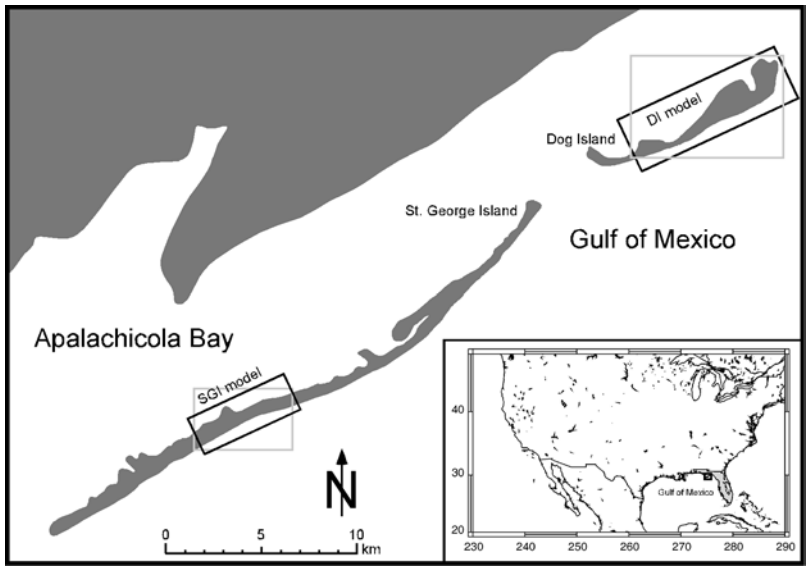

Fig. 1 Map of St. George Island and Dog Island. *Light box* on St. George Island marks locations of Figs. 3, 5, and 7. *Light box* on Dog Island marks locations of Figs. 4, 6, and 8. *Dark boxes* indicate boundaries of 3-D models. *Inset*: *Box* shows location of larger map; *gray shading* indicates state of Florida

study as they share reasonably similar geologic and hydrologic patterns, but differ significantly in the level of anthropogenic impacts. The primary driving factors behind lens development on these islands appear to be: (1) spatial and temporal variations in recharge, (2) human development and water use, and (3) coastal erosion (Schneider and Kruse 2003). In this study, the importance of selected factors were studied with groundwater flow models. Most notably, the modeling presented here shows that the impact of coastal erosion and island migration on freshwater lens development may be significant; these results may be applicable to other barrier islands experiencing erosion.

Variable-density numerical flow models were developed using SEAWAT (Guo and Langevin 2002). While analytical models of freshwater lenses (e.g., Vacher 1988a) are straightforward and useful for the representation of simple spatial variability, numerical models provide the flexibility needed to explore complex spatial patterns and to consider temporal response to transient processes.

Freshwater lens development

Theory

Dupuit-Ghyben-Herzberg (DGH) theory postulates that an ideal freshwater lens (i.e., within a homogenous, isotropic, infinite-strip island) is symmetrical about the island's center and the depth to the freshwater-saltwater interface is directly proportional to the elevation of the water table above mean sea level (Hubbert 1940). The thickness of the lens depends on the ratio of the recharge rate (R) to hydraulic conductivity (K) of the aquifer (larger R/K yields thicker lens) and the size of the island (larger islands develop thicker lenses). The size of the transition zone separating fresh and salty groundwater (not part of the DGH model) is dependent on aquifer parameters and tidal range (Cooper 1959). In general, thicker transition zones develop in high K, low storage media, and in areas with greater tidal range.

Vacher's (1988a) analytical models demonstrate that K or R variability across the island results in an asymmetric lens, with maximum lens thickness skewed toward the region with greater R/K. Vertical K variability also affects the shape of the lens—a high K unit at depth promotes mixing of fresh and salty groundwater, limiting the depth of freshwater lens development while creating a thick transition zone. An impermeable unit at depth impedes vertical flow of groundwater, and results in higher than usual water table elevations, although total lens volume is less (Vacher 1988a).

Geologic controls

Several articles document geologic control on fresh groundwater distribution in coastal barrier islands (e.g., Harris 1967; Fetter 1972; Kidd and Planert 1985; Simmons 1986; Collins and Easley 1999; Anderson et al. 2000). However, reasonably consistent patterns have not been identified. This is due at least in part to variability in barrier island stratigraphy. Barrier island systems incorporate numerous depositional environments, including beaches and dunes, washover fans, marshes, tidal flats, tidal inlets, and the bay/lagoon separating the island from the mainland (Davis 1997). Resulting stratigraphy is some combination of sand (beaches, dunes, washover fans) and finer grained sediments (tidal flat, marsh, and bay deposits). These siliciclastic sediments are associated with a low overall range of K values.

Examples of the hydrostratigraphic complexity on barrier islands include a study by Collins and Easley (1999) showing a highly heterogeneous lens in sand permeated by semi-horizontal discontinuous thin silt and clay layers. Fetter (1972) described a case where the lens is thickened due to a lower K unit (~20 m/day, Cretaceous sediments) underlying the surficial glacial

 DOI 10.1007/s10040-005-0442-9

aquifer (K~45 m/day) on the South Fork of Long Island. In a few cases, the freshwater lens does appear to be effectively truncated by a thick continuous clay layer, presumably associated with a very low K (e.g., Kidd and Planert 1985; Simmons 1986).

Terrain effects

Terrain (this term is used here to describe elevation and surficial geomorphology) and vegetation variability can strongly influence recharge patterns on small islands (Wallis et al. 1991; Whittecar and Johnson 1990; Whittecar and Johnson 1991; Vacher and Quinn 1997; Schneider and Kruse 2003). While long-term precipitation (P) patterns are probably fairly uniform within a small island, R is often highly spatially variable. Marshes and ponds produce excess evaporative loss, and dense vegetation results in excess transpiration. In contrast, dune topography reduces evapotranspiration (ET). Human development can further alter these R patterns in a variety of ways, particularly through reduction of R by paved surfaces and alterations of vegetation and terrain patterns.

Unequal sea level and tidal effects

On barrier islands, a significant difference in effective mean sea level between the bay and the ocean can result in an asymmetric lens (e.g., Urish 1980; Vacher 1988b; Urish and Ozbilgin 1989). This process may be important on small (few 100's meters) strip islands with relatively low R/K (Vacher 1988b; Urish and Ozbilgin 1989). Unequal sea level effects may be important on the thinnest parts of St. George and Dog Island (Schneider and Kruse 2003), but are not addressed in the island-scale models of this study.

On high K carbonate islands, tidal mixing of fresh and salty groundwater is a significant force in the loss of fresh groundwater to the mixing zone. Tidal efficiency (the degree to which the tidal signal is propagated inland) in the relatively low K materials that compose siliciclastic islands is generally low, and there is a weak correlation between tidal range and mixing zone thickness.

Transient effects

Small islands experience a wide range of short and long-term climate patterns, and naturally change size, shape and position over time. The groundwater system responds with a lag time based on the range and distribution of K. Seasonal and interannual variations in fresh groundwater inventories on islands with a high K can be substantial, due in large measure to variations in rainfall, which are superimposed on the approximately constant rate of tidal mixing within the groundwater body (e.g., Vacher and Quinn 1997; Ayers 1998).

Seasonal changes are likely to be less pronounced on sandy barrier islands where K values are commonly much lower, and lag times are correspondingly larger. For example, there does not appear to be significant seasonal change in lens volume on St. George Island (Schneider and Kruse 2003). However, sandy barrier islands naturally change size, shape, and position over relatively short durations; some are migrating landward at rates of several meters per year (Davis 1994). Many small islands of both types have experienced considerable anthropogenic alterations (i.e., man-made inlets and canals) in recent years (e.g., Langevin et al. 1998). Where these changes have occurred, particularly in low K materials, transient lens configurations may represent long-term responses to a variety of triggering processes.

Dog Island and St. George Island

Dog Island and St. George Island are located ~5 km offshore of the Florida panhandle in the northeastern Gulf of Mexico (Fig. 1). Dog Island is a "drumstick" shaped barrier island (~100–2,000 m × 10 km) while St. George Island is a strip barrier island (~250–1,500 m × 30 km). The terrain of a typical across-the-island transect consists of dunes along the Gulf coast and salt marshes along the Bay shore, with various trees and shrubs populating the land in between (Livingstone 1983).

On both islands, 5–10 m of fine to coarse quartz Holocene sand overlies a thin (~0.5–2 m) Pleistocene layer described as clay, silt, or silty-sand (Schnable 1966). This material is underlain by an additional 5–6 m of Pleistocene fine to coarse sand on St. George Island. The underlying Pliocene Intracoastal Formation is characterized by sandy and clayey consolidated biogenic limestone and poorly consolidated calcarenites (Otvos 1985). The Pliocene contact slopes toward the gulf from a depth of 12–15 m on St. George Island and 9–12 m on Dog Island.

Dog Island has experienced significant erosion, as much as 2.5 m/year between 1856–1979 along its Gulf coast, while elongating through the process of spit migration (Donoghue and Tanner 1994). St. George Island has experienced erosion along its entire Gulf shoreline during the past century as well, with rates ranging from less than 1 m/year to over 2 m/year (Schade 1986). Apalachicola Bay shorelines on both islands have also been retreating, with rates averaging just under 1 m/year (Donoghue and Tanner 1994).

Access to Dog Island is by ferry only, which has limited development to relatively few (~100), predominantly seasonally occupied homes. Most of these homes are along the Bay and Gulf coast, where shallow wells provide the water supply and septic systems are used for waste disposal.

Development on St. George Island is more variable. The eastern portion of St. George Island is a State Park; the remainder of the island has been developed rapidly over the past ~25–30 years following the construction of a bridge to the mainland. Heaviest development has occurred in the central area surrounding the bridge, shown on Fig. 2. Four island-parallel roads allow homes to be densely distributed throughout this portion of the island.

 DOI 10.1007/s10040-005-0442-9

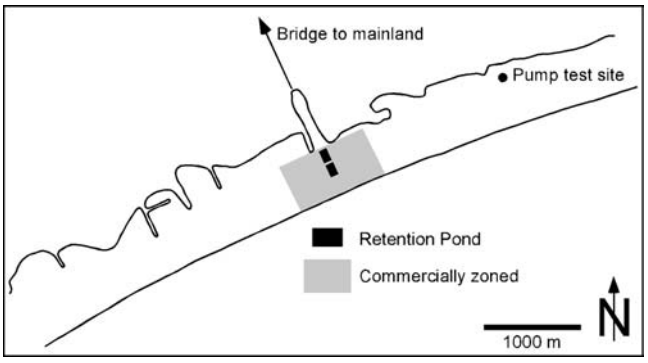

Fig. 2 Map of central portion of St. George Island (location shown on Fig. 1, *light box* on St. George Island). Location of pumping test also shown

The area several blocks to the east and west of the location where the bridge joins the island is commercially zoned (Fig. 2); here anthropogenic effects are expected to be greatest. Water demand on St. George Island far exceeds the supply potential from the freshwater lens, and an aqueduct supplies water from a well field on the mainland. Some on-island shallow wells (3–5 m) are used for lawn and garden irrigation. Although a few developments have a central wastewater treatment facility, septic systems are the primary mode of waste disposal on St. George Island.

The domestic water supply (via aqueduct) on St. George Island is a potentially significant source of artificial recharge to the freshwater lens. In 1998, the island consumed ~600,000 m^3 of aqueduct water, the bulk of which was recharged to the aquifer through household septic systems. Assuming all recharge occurred on the developed (non-State Park) portion of the island (~17.5 km long by ~500 m wide) this translates to ~0.07 m/year of artificial recharge. Average precipitation recorded during the period from 1993–2000 is ~1 m/year (Fig. 3). Depending on the percentage of precipitation which goes to recharge the freshwater lens, the artificial recharge is at least 7% of the natural recharge (assuming recharge = precipitation), and could be as much as ~25% (assuming recharge ≅ 1/4 precipitation) or more. Other anthropogenic activities also appear to have a significant effect on the freshwater lens morphology (Schneider and Kruse 2003). Alterations of vegetation and elevation during development, such as clearing vegetation, filling in marshes, and erosion of dunes affect recharge.

Field data: results and interpretation

Geophysical surveys of freshwater lens volume

Figures 4 and 5 show the results of electromagnetic (EM) surveys performed to determine the spatial and temporal variations in the freshwater lenses of Dog Island and St. George Island. The EM data were inverted in order to estimate the depth of the interface between fresh and saline groundwater (Schneider and Kruse 2003). By mapping the base of the lens, an estimate can be made of the total volume of the freshwater lens and longer-term (seasonal to decadal) variability in the lens shape and volume (e.g., Lloyd 1984), which is the focus of this study. The reader is referred to Schneider and Kruse (2003) for a more complete discussion of the geophysical methods and interpretation, and the benefits and drawbacks of this approach in studying these freshwater lenses.

Key features on both islands include: (a) the lenses are asymmetric—thicker toward the gulf side, much thinner on the bay side; (b) the lenses extend to depths of 20 m or more, well into the Pliocene limestone; (c) lens morphology varies along the island, particularly in the narrower and more developed zones on St. George Island; (d) seasonal variations in lens volume are small. Freshwater lens morphology is clearly more complicated than can be attributed to a homogenous distribution of aquifer parameters and coastal and recharge boundary conditions.

Hydraulic conductivity (K)

The K of the Holocene sands of St. George Island has been previously evaluated through several methods. Corbett et al. (2000) use equations presented by Ferris (1963), which assumes an unconfined aquifer, to estimate K of sands from measured tidal variations in water table elevations at three wells located in the state park, ~1, 40 and 100 m from the bay shore. By assuming a thickness for the aquifer of 8.5 m, and a storativity of 0.25, they arrive at K=20, 70 and 180 m/day, respectively. Corbett et al. (2000) estimate their uncertainty at approximately half of the computed values (i.e., ±50%). K appears to increase

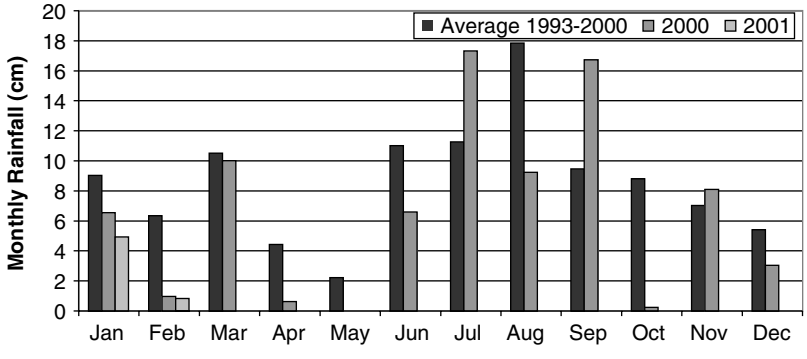

Fig. 3 Monthly rainfall recorded along bridge to St. George Island. No data after Feb. 2001

DOI 10.1007/s10040-005-0442-9

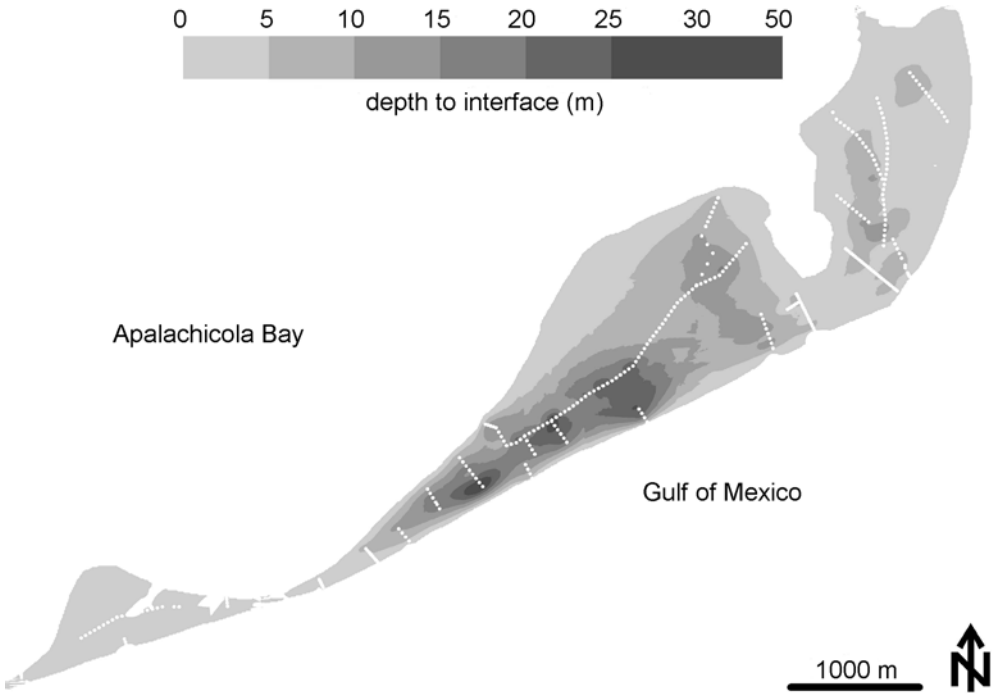

Fig. 4 Results of EM surveys of Dog Island showing depth to interface (location shown on Fig. 1, *light box* on Dog Island). *White dots* indicate locations where data were collected

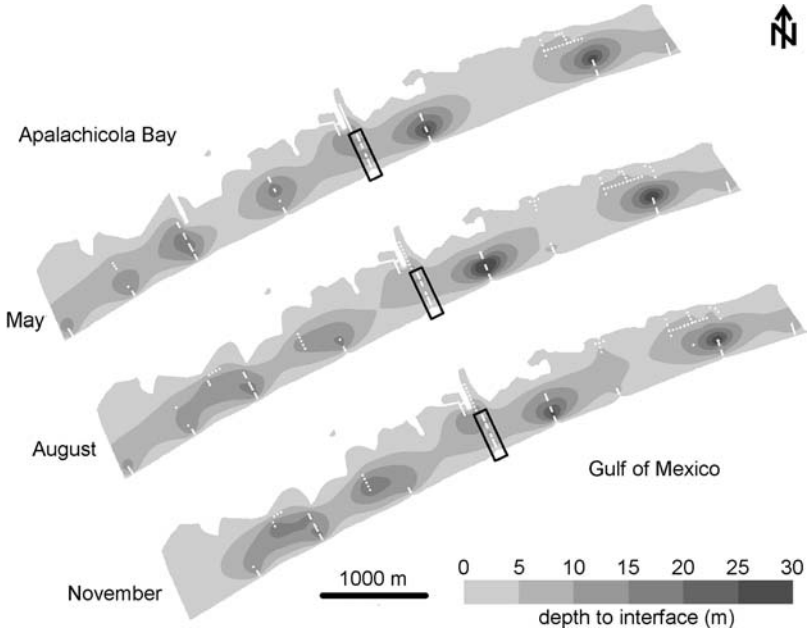

Fig. 5 Results of EM surveys showing depth to the interface of central portion of St. George Island (Fig. 1, *light box* on St. George Island). *White dots* indicate locations where data were collected. *Patterns* shown in areas with no data coverage are artifacts of the contouring process

with increasing scale of measurement (greater propagation distance for the tidal signal).

Ruppel et al. (2000) use an analytical method presented by Urish and Ozbilgin (1989), which also assumes an unconfined aquifer, to interpret three sets of head measurements conducted at the Corbett et al. (2000) study site on St. George Island. By assuming a thickness and storativity (also 8.5 m and 0.25, respectively) for the aquifer, they calculate a range of ~3–13 m/day for the K of these sediments, over the tens of meters spanned by these wells.

Corbett et al. (2000) also provide estimates of K from tracer experiments conducted at several locations on St. George Island. These experiments determine the horizontal transport rate (v) between wells tens of meters apart. By measuring the hydraulic gradient (i) between the wells, and the porosity (n) of the sediments (estimated in their study by gravimetric methods), K can be calculated from Darcy's Law ($K=vn/i$). By this method, a range for K was estimated at 2.7 to 75 m/day.

In this study, a traditional pumping test was undertaken at another site on St. George Island (Fig. 3), where a fully screened well and 7 piezometers were located ~120 m landward from the bay shore. Even at this distance, groundwater tidal fluctuations obscured the response after early

 DOI 10.1007/s10040-005-0442-9

time (10's of minutes). Fitting the early time portion of the time-drawdown curve to the Theis curve yielded K values of ~5–10 m/day for a surficial aquifer 10 m thick. (The Theis method certainly represents an over-simplification for this setting, however the limited data set did not warrant the use of more complex methods). At the test site freshwater extends to a minimum of ~7.5 m as determined from water conductivity measurements, and local geophysical surveys indicate the lens is probably not much more than 10 m thick (Schneider and Kruse 2003). Another pumping test performed by a private consulting firm at a site to the west of the area shown in Fig. 3 yielded a value for K of ~48 m/day (Mortensen Engineering, Inc. unpublished data). The pumping test K estimates sample a similar length scale (tens of meters) to the tracer studies.

Observed K clearly tends to increase with increased scale of measurement, but also varies between methods sampling reasonably similar volumes. The latter is best seen in a comparison of the results of Corbett et al.'s (2000) and Ruppel et al.'s (2000) analyses of head measurements from identical wells on St. George Island. The two groups arrived at quite different ranges of K values. The probable range of K for these islands was explored further in the groundwater models, as discussed below.

Dispersivity

Corbett et al. (2000) provide estimates of longitudinal dispersivity (α_L), based on in-situ geochemical tracer experiments for two bay-side sites on St. George Island. As expected, α_L values were highly scale-dependent (e.g., Fetter 1993). At one of Corbett et al.'s (2000) sites, the tracer flow path was 67 m, and α_L estimates range from 0.1 to 0.5 m. At the second site, the scale of observation was 7 m, and α_L estimates are an order of magnitude smaller (0.03–0.04 m).

Recharge

Average monthly precipitation (P) measured at the weather station on the bridge to St. George Island for the period of 1993–2000 (weather station installed in 1993) is shown in Fig. 3. Total average yearly P is ~1 m. Monthly P during the study period (Jan. 2000 through Feb. 2001) is also plotted in Fig. 3. While the monthly P during the study period differs from average P during some months, the general pattern is the same with greatest P during the summer months.

Figures 6 and 7 show the Gulf sides of St. George and Dog Islands are characterized by relatively unvegetated dunes, while the Bay sides of these islands are characterized by low-lying marshes and pine forests. Interception (rain caught by tree canopy and litter and evaporated back into the atmosphere) can account for 20–25% of total P in coniferous forests (Dunne and Leopold 1978). Interception (I) on the relatively sparsely vegetated dunes is probably much less. Potential ET, calculated by several methods (Thornthwaite and Blaney-Criddle) based on average monthly air temperature, is ~1 m/year, and potential ET expected for this region based on US weather service pan evaporation data is ~1.2 m/year (Dunne and Leopold 1978). Runoff is probably insignificant on these islands because rainfall readily infiltrates the ground, so R ($=P-ET-I$) can theoretically range from 100% precipitation (~1 m/year) (i.e., no I or ET) to values as low as ~ −0.4 m/year ($I+ET>P$). ET is expected to be strongly seasonal (potential ET is very high in the summer and much lower in the winter) and may have an even greater effect on seasonal patterns of recharge than monthly rainfall variability.

Groundwater modeling

Variable density numerical flow models were developed using these field observations to investigate the importance of spatial and temporal variability in R, anthropogenic impacts, and coastal erosion on the patterns of fresh groundwater occurrence on these two small sandy barrier islands. Other natural processes such as tidal oscillations, waves, sea-level rise, and sea-level differences between ocean and landward shores surely also effect the freshwater lenses of these islands, but they are beyond the scope of this paper. This study addresses variability in total lens thickness, so the focus is on the base of the lens. A summary of important parameters and other settings utilized in the models is shown in Table 1.

Table 1 Parameters and other settings used in the SEAWAT models

MODFLOW	
Hydraulic conductivity	
Horizontal	5 m/day
Vertical	5 m/day
Recharge	
minimum	−10 cm/year
maximum	43 cm/year
average	~12.5 cm/year
Porosity	0.35
Specific yield	0.25
Flow package	BCF
Solver package	PCG2
MT3DMS	
Dispersivity	
longitudinal	1 m
transverse	0.1 m
Concentration of seawater	35 kg/m^3
Density-concentration coupling factor, dρ/dC*	0.71
Advection solution scheme	MOC
Courant number	1.0
Solver for dispersion and source/sink mixing	GCG

*This is specified by SEAWAT

 DOI 10.1007/s10040-005-0442-9

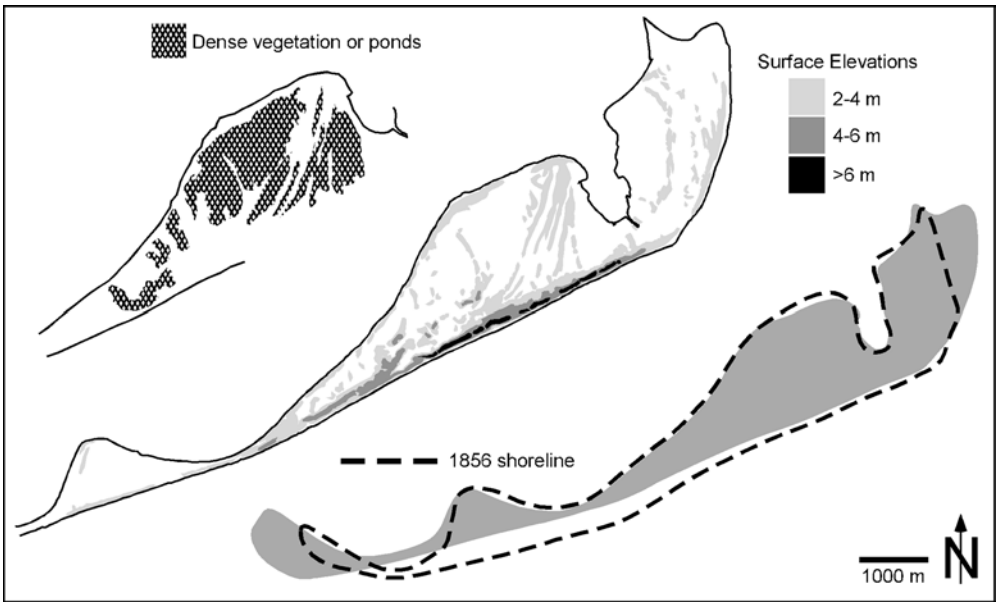

Fig. 6 Patterns of vegetation and topography and recent history of sedimentation and erosion on Dog Island. Location shown on Fig. 1

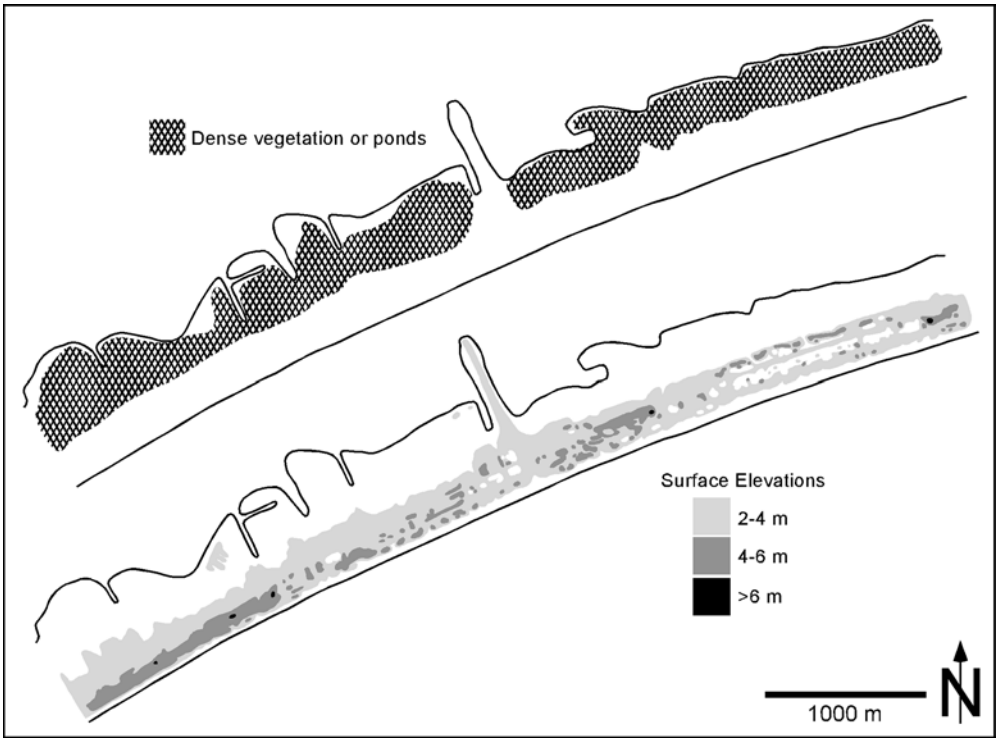

Fig. 7 Patterns of vegetation and topography on the central portion of St. George Island. Location shown on Fig. 1

Code

The numerical modeling code chosen for this study is SEAWAT (Guo and Langevin 2002), which was developed specifically for modeling variable-density groundwater systems such as coastal aquifers. SEAWAT couples MODFLOW (McDonald and Harbaugh 1988) and MT3DMS (Zheng and Wang 1998) to simulate three-dimensional variable-density groundwater flow. SEAWAT reads standard MODFLOW and MT3DMS input files, so it is possible to create models and interpret results using commercially available graphical user interface codes, a significant advantage over previously available coastal aquifer numerical models such as SHARP (Essaid 1990).

Parameters

Hydraulic conductivity

Freshwater lens volume is controlled to first order by the ratio R/K, as described by the DGH equations (Hubbert 1940). Flow models are thus inherently non-unique: an

 DOI 10.1007/s10040-005-0442-9

increase in R can be offset by an increase in K. The validity of any model can then only be assessed on the basis of the plausibility of the assumptions of R and K, based on existing hydrologic and geologic evidence. There is generally good agreement among the methods discussed above that K lies in the range of 3–75 m/day for flow scales of tens of meters. Several lines of evidence suggest that spatial form of the lenses on Dog Island and St. George Island are controlled primarily by the pattern of R, rather than by spatial variations in K (Schneider and Kruse 2003). The pattern of R appears to be controlled by the natural patterns of both terrain and vegetation, which in some areas have been altered by human development to the extent of affecting the spatial form of the freshwater lenses.

The principal relevant observations with respect to potential patterns of K on these islands are: (1) the lenses are very thin (<6–8 m) on the islands' bay sides, and thicker on the ocean sides; and (2) the lenses extend to depths of tens of meters. To explain (1) based on K variability would require, exclusively on the bay side of the islands, either a (semi) confining unit at depths less than 6–8 m, or a highly permeable unit below these depths. Neither scenario is compatible with cores (Schnable 1966), which indicate the only significant contact in the uppermost 30 m is the top of Pliocene limestone that lies at 9–12 m depth and extends beneath both bay and ocean sides. Geophysical surveys (seismic and ground penetrating radar) targeting stratigraphic horizons show no distinct layering that might serve as a semi-confining unit in the uppermost 10 m on bay or ocean sides. The only other way to generate the inferred asymmetry based on K variability is to assume a significant lateral increase in permeability across the island from the Gulf to the Bay side. K would need to be ~1–2 orders of magnitude larger on the Bay side (Ruppel et al. 2000); this is highly unlikely given that core descriptions are consistent across the island. Radar velocities (sensitive to porosity in the uppermost few meters) also do not vary significantly from bay to ocean side.

It is possible, even probable, that the Pliocene limestone has a significantly higher K than the overlying sediments. Because the limestone-sediment contact dips gently seaward beneath the islands, however, the contrast alone cannot explain the dramatic difference in lens thickness on bay and ocean sides. Groundwater flow models incorporating a K contrast at the limestone-sediment contact could be found that yield results similar to those with a uniform K shown in discussions below. Thus the data are compatible with, but do not require, a K contrast at this geologic discontinuity. (The observation that the lenses extend well into the limestone does preclude a sharp drop in K or an extreme rise in K in the limestone.) For simplicity, then, a uniform K value is assumed in the suite of groundwater flow models shown here.

Preliminary flow models of these islands showed that any K values except those at the low end of the observed range (~3–75 m/day) yielded an aquifer thickness much thinner than that inferred from geophysical data, even when very high R rates (e.g., 50–100% of precipitation) were used. A value of 5 m/day was determined to yield good results for a reasonable range of R (e.g., average net R of 10 to 25% of precipitation). Models with anisotropic K values (vertical K=0.5 m/day) were tested during the calibration process, but an isotropic K yielded better model results.

Dispersivity

The geophysical surveys, calibrated against direct water sampling, yield estimates of the local depth to the freshwater/saltwater mixing zone (e.g., Figs. 4 and 5), but cannot be used to determine the thickness of the mixing zone. As only isolated constraints exist on the thickness of the mixing zone, appropriate dispersion coefficients cannot be estimated for the freshwater lens as a whole. The total scale of flowpaths on these islands is hundreds of meters, roughly an order of magnitude larger than the scale on which dispersivities were measured by Corbett et al. (2000). Assuming appropriate α_L values for these models are likely to be an order of magnitude larger than that determined by Corbett et al. (2000) for their larger site (0.1–0.5 m), α_L is set to 1 m. Models with a α_L of 1 m produce a mixing zone on the Bay side of the island ~8–10 m thick. Groundwater samples collected in the subsurface at one site on the Bay side of the island indicate a mixing zone at least ~6 m thick.

Transverse (perpendicular horizontally and vertically) dispersivity (α_T) could not be estimated by Corbett et al. (2000) since tracers never consistently appeared in wells out of line with the flowpath between the injection well and the coast. This suggests that α_T must be relatively small. In these models α_T is set at 0.1 m; other studies have suggested α_T is typically about an order of magnitude smaller than α_L (Fetter 1993).

As will be discussed further below, the targeted depth in the groundwater models is the center of the transition zone. Clearly, the thickness of the transition zone is sensitive to the choice of dispersivity, but the location of the center of the transition zone should not be significantly affected. Model runs with different values of dispersivity did not exhibit any noticeable difference in the center of the transition zone, thus errors resulting from this choice should have a minimal impact on the conclusions reached from the modeling exercises.

Recharge

A good correlation emerges between freshwater lens thickness (Figs. 4 and 5) and the combined patterns of vegetation and elevation (Figs. 6 and 7) on these islands (Schneider and Kruse 2003). The obvious inference is that the vegetation and elevation patterns affect lens thickness by creating spatially variable R patterns. Greater evaporation in low areas, and greater transpiration and interception in more vegetated areas, reduces R and results in a thinner lens. While the potential magnitude of these reductions to the water budget can be calculated, actual data on the spatial and temporal variability of these components were not available. Therefore, for simplicity, these components were not individually included in the

 DOI 10.1007/s10040-005-0442-9

groundwater models. The R applied to the models is the net R ($=P-\mathrm{ET}-I$); all mentions of R below are referring to the net R.

With the assumption of uniform K, a spatially variable R is required to create the complex freshwater lenses observed on Dog Island and St. George Island. R is only applied to the island portion of the models. Monthly P during 2000 (when temporal data on the St. George Island lens was obtained) shows more variability than the average monthly P over the last 8 years. However, even during 2000, lens morphology inferred from geophysical data remained largely unchanged over the course of the year (Schneider and Kruse 2003; Fig. 5). While measured water levels clearly were affected by rainfall patterns, overall lens morphology and thickness was not. Thus, in the models described below, seasonal variability is neglected unless otherwise specified; R is assigned as a fixed value per day.

In the models presented here, the average R applied to the islands is approximately 10 to 15% of average yearly P. Local recharge rates range from +43% to −10% of the average yearly P. As described above, potential losses due to interception and ET (as much as 1.45 m) do indeed exceed average rainfall totals (~1 m), and the range of losses required in the calibrated models (57–110% of P) appears to be reasonable. Modeling of spatial and seasonal patterns of R is discussed in more detail below.

Other parameters

As with K, other aquifer parameters were also considered to be homogeneous throughout the island. Porosity of St. George Island sediments was measured gravimetrically by Corbett et al. (2000) to be ~0.3–0.35. In the models, porosity was specified as 0.35 and specific yield as 0.25. These are both reasonable values for fine sands (Domenico and Schwartz 1998).

Initial conditions

Initial conditions were modeled assuming all groundwater salinities at the level of seawater (35 kg/m^3). As the freshwater lens develops due to the introduction of fresh R over the island, total mass in the model is gradually reduced until the total mass and freshwater volumes in the model domain reach steady-state. Typical model runs required 200–500 years to arrive at steady state. The steady-state heads and concentrations were then used as the starting point to evaluate the effect on lens development of some of the natural and anthropogenic processes occurring on these islands.

Boundary conditions

Figure 8 shows a conceptual model of the boundary conditions for the groundwater models. Vertical model boundaries (offshore of the island), as well as uppermost layer cells representing open seawater, are constant head boundaries with a head of zero. The salt concentration along these boundaries is specified as 35 kg/m^3. As a result, any

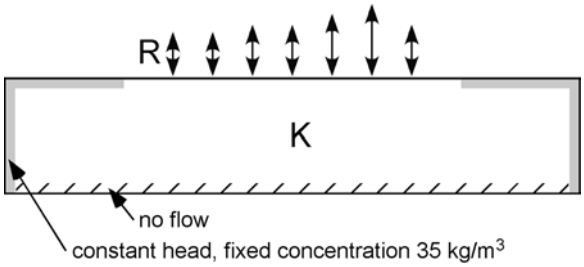

Fig. 8 Conceptual model. *Double arrows* represent net recharge (precipitation minus evapotranspiration)

water that enters the model in order to maintain the constant head has a concentration of 35 kg/m^3. However, these cells can have a salt concentration less than 35 kg/m^3 if freshwater head on the islands is sufficient to drive fresh groundwater offshore. For models that capture only a portion of the island, model boundaries are set approximately perpendicular to the local strike of the island and the boundaries cutting across the island are considered to be no-flow. Such a boundary condition implies groundwater flow perpendicular to the long axis of the island, which as shall be seen is not always the case, but the errors introduced by this assumption should only be large near the edges of the model. The base of each model is also a no-flow boundary, which is valid as long as it is at least several layers deeper than the base of the freshwater lens (Chris Langevin, U.S.G.S., personal communication, 2001).

Model scenarios

As stated above, the freshwater lens development on Dog Island and St. George Island appears to be controlled principally by the patterns of vegetation and terrain, which in turn controls R (Schneider and Kruse 2003). Selected additional stresses (i.e., wells), time varying stresses (i.e., seasonal recharge patterns), and changing boundary conditions (i.e., island erosion) may also be important to lens development on these islands. These are examined in turn below.

Lens morphology dependence on recharge

To test the hypothesis that spatial patterns of R are the dominant control on the freshwater lens morphology on these islands (Schneider and Kruse 2003), three-dimensional, steady-state models of portions of Dog Island and St. George Island were created. The R applied to these models was adjusted to create models that match the geophysically inferred freshwater lens. A model of most of Dog Island (Fig. 1) was created using a grid of 100 m by 100 m, except within the area of the island, where the cells are 50 m (y direction) by 100 m (x direction), and with 10, 4-m-thick layers. Finer model discretization would have required prohibitively long computer run-times.

To assess numerical dispersion arising from the coarse discretization, a suite of 2-D models were run, with uniform cell sizes ranging from 1–100 m (all other parameters identical). Models run with no dispersion ($\alpha_L=\alpha_T=0$)

 DOI 10.1007/s10040-005-0442-9

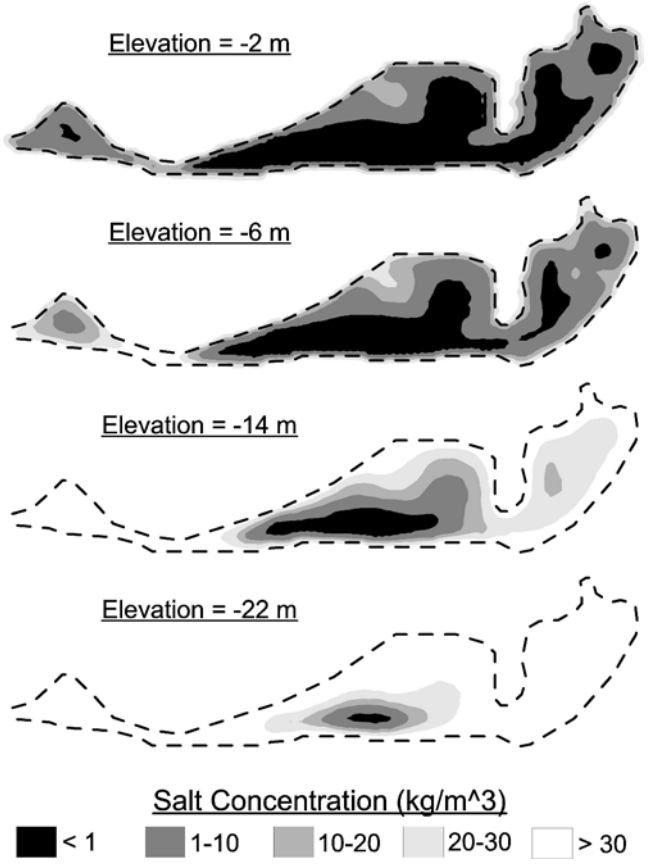

Fig. 9 Results of the 3-D model of Dog Island (Fig. 1, *dark box* on Dog Island)

yielded a fairly sharp interface (mixing zone one or two cells thick) regardless of grid spacing. Models with non-zero dispersion show similar freshwater lens and mixing zone thicknesses at large and small grid spacing. Thus, the chosen grid represents a reasonable compromise between model run time and limited numerical dispersion.

Any model cell more than five cells away from the islands shore was set to no-flow. It was assumed that the interface depth derived from the EM surveys corresponds to the depth at which the salt concentration is 50% that of seawater. Concentration targets equal to 17.5 kg/m^3 were inserted into the model at the depth of the "interface" from the EM surveys (seawater concentration = 35 kg/m^3, freshwater = 0 kg/m^3). Sixty-three of the data points from the Dog Island EM surveys (shown in Fig. 4) were chosen for this comparison.

The metric used to evaluate the match between the model and the geophysically inferred lens is the absolute residual mean. The residual at each target can range from −17.5 to 17.5 kg/m^3, with an optimal value of 0 kg/m^3. The absolute value of all residuals is then averaged to obtain the absolute residual mean, which can range from 0–17.5 kg/m^3. The closer this value is to 0 kg/m^3, the better the model simulates the observed data. Optimizing the concentration at these targets is similar to matching calculated and observed lens thickness, in that residuals increase for models in which the transition zone is too shallow or too deep.

The resulting distribution of groundwaters through several layers of the Dog Island model is shown in Fig. 9. The recharge array used in this model is shown in Fig. 10. This configuration of R yields an absolute residual mean concentration of ∼4.4 kg/m^3 for the 63 target locations. That is to say, the average absolute value of the difference between 17.5 kg/m^3 and the concentrations in the model at the location and depth of the calibration targets was ∼4.4 kg/m^3. Based on this, it appears the model can accurately simulate the inferred freshwater lens (Fig. 4) assuming plausible variations in R, which are correlated with patterns of vegetation and elevation (Fig. 6).

A model of the central portion of St. George Island (Fig. 1) was similarly created to test the hypothesis that spatial variability in R may be the primary control on lens thickness. This area was discretized into a uniform grid of 40×40 m, also with 10, 4-m-thick layers. Any model cells more than five cells away from the shore were set to no-flow. As with the Dog Island model, this discretization of the model area balances resolution with model run-time. This model was also attempting to simulate the depth of the EM derived freshwater-saltwater mixing zone; 31 of the data points from Fig. 5 were chosen for this purpose. R was adjusted throughout the model until the modeled freshwater lens closely approximated the inferred lens (average absolute residual concentration of 3.7 kg/m^3 for the 31 targets locations). The resulting salinity of groundwater through several layers is shown in Fig. 11, and the recharge array used is shown in Fig. 12. This model also accurately simulates the inferred freshwater lens asymmetry (Fig. 5) using recharge variability correlated with patterns of vegetation and elevation (Fig. 7).

Both the Dog Island and St. George Island models demonstrate that variations in R that correlate with vegetation patterns can produce the inferred freshwater lens morphology. In both models, the largest values of R are distributed beneath the dune line on the Gulf side of the island (Figs. 5 and 7). Negative values of R are required to fit lens thickness in areas on the back of the island where extensive marshes, ponds, and forests occur. As stated above, potential losses of recharge due to interception and ET can potentially exceed average P received by these islands. Chloride concentration of groundwaters collected from shallow wells ∼100 m inland from the Bay side of the island are significantly higher (up to 1,000 ppm) than chloride found in a rainwater sample (∼15 ppm), which suggests that ET losses are indeed very large in these zones.

For models of both islands, the total lens thickness in most areas was reproduced, and the general pattern of fresh groundwater occurrence throughout these islands was well reproduced. However, the maximum lens thickness on each island inferred from geophysical data could not be simulated in the groundwater models. Locally, inferred lens thickness is as much as 25–30 m in some areas, but maximum lens thickness in the models is only ∼20 m. This discrepancy may be due to the relatively coarse discretization of the model domains (necessary to model these large areas) and other simplifications (i.e.,

 DOI 10.1007/s10040-005-0442-9

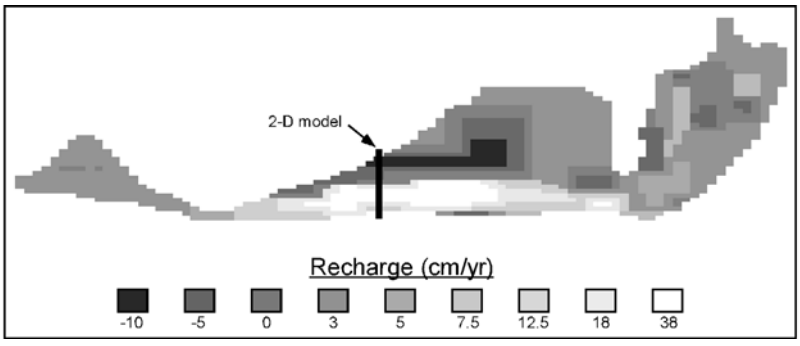

Fig. 10 Recharge array used to produce Dog Island model results shown in Fig. 9

assignment of relatively few recharge zones with sharp boundaries, homogenous aquifer parameters). In addition, the sensitivity of resistivity and EM ground conductivity readings (used to infer pore water salinities) decrease with depth; thus lens thickness estimates are most uncertain where the lens is thickest. Finally, the continuous erosion of the islands and/or sea level rise over the last century may also result in a thicker than expected lens (as the lens lags behind changes in boundary conditions). A model addressing erosion is described below.

Seasonal variability of recharge on St. George Island

A suite of repeated EM and resistivity surveys of lens geometry were collected on St. George Island through the wet and dry seasons of 2000 (Schneider and Kruse 2003). These surveys indicate little if any seasonal variability in freshwater lens morphology through the year. However, the surface of these lenses (i.e., the water table) responds to rainfall events and varies throughout the year with wet and dry seasons (Corbett et al. 2000; Ruppel et al. 2000). The absence of lens response to significant seasonal variations in rainfall suggests that the base of the lens only responds to longer scale R variations (e.g., decadal scale drought cycles).

A model incorporating plausible seasonal variations in rainfall and ET estimates supports this supposition. The model was run through a single year with a separate value for R assigned to each month. The initial heads and concentrations were taken from the calibrated 'yearly average' model described above for the central portion of St. George Island (Fig. 11). Monthly R in the five recharge zones (Fig. 12) was determined as follows. The average monthly P (for period from 1993–2000) was first reduced by 5–20% (higher values in lower recharge areas) representing interception by vegetation (as previously reported, interception can be as high as 20–25% in coniferous forests; I is presumably lower in other areas of the island). It was then assumed that the ET each month is a fixed fraction of the potential ET for that month, computed from the Thornthwaite formula. This fraction is fixed throughout

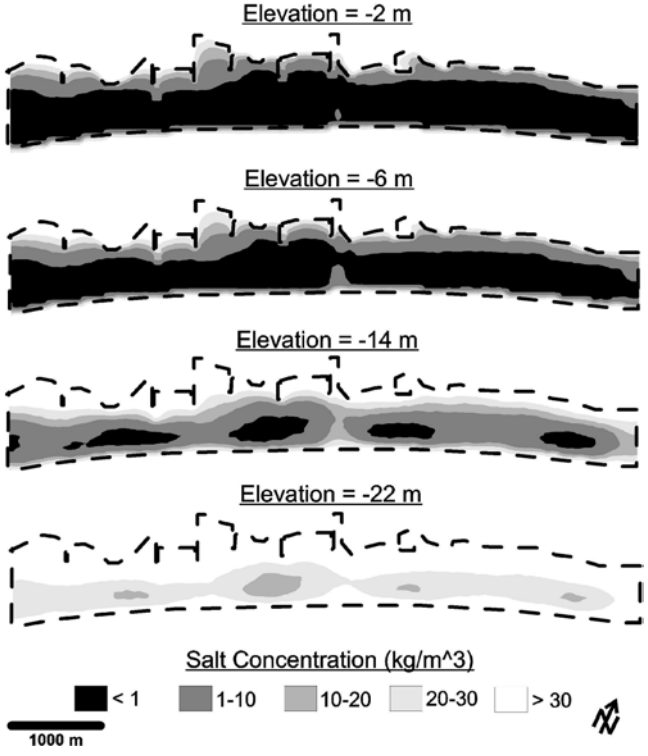

Fig. 11 Results of the 3-D model of the central portion of St. George Island (Fig. 1, *dark box* on St. George Island). *Dashed line* defines the extent of the island within this modeled area

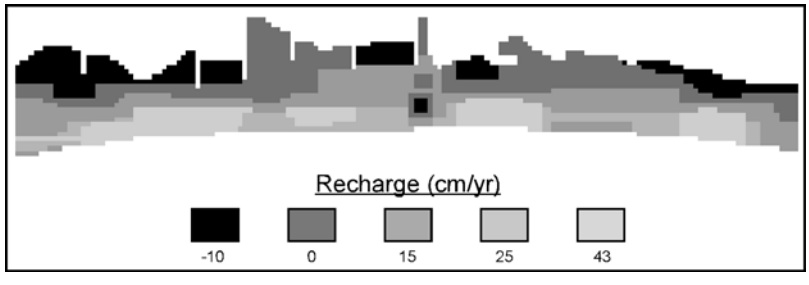

Fig. 12 Recharge array used to produce St. George Island model results shown in Fig. 11

DOI 10.1007/s10040-005-0442-9

the year for each zone so that the total of all the monthly R values roughly equals the annual R used for the model shown in Fig. 11. Because potential ET (and hence assumed ET) is so much greater in the summer months, R is actually highest in the winter months, even though P is lower.

The impact of this monthly variability in R was evaluated by comparing the average concentration at the 31 targets used to develop the steady-state version of this model (Fig. 11). Average concentrations did change in a pattern consistent with the R pattern (i.e., concentration became lower when R was greater, meaning the depth to the 'interface' increased), but only by very small amounts ($\sim$0.4 kg/m^3 total range). This is consistent with the lack of temporal variability inferred in the lens on St. George Island based on geophysical data. Presumably, the much lower hydraulic conductivity on this island, compared to that of carbonate islands, attenuates in the base of the lens seasonal variability observed in the surface of the lens.

Impact of aqueduct water and development on St. George Island

In the calibrated models, the recharge rates on St. George Island (Fig. 12) are $\sim$5–10 cm/year larger than those used for many comparable areas on Dog Island (Fig. 10) (e.g., the relatively elevated and sparsely vegetated portions of St. George Island require R=25–43 cm/year, while on Dog Island rates are only 12.5–38 cm/year). While the assumed recharge arrays are by no means unique (i.e., other patterns of similar recharge rates could obtain a comparably good calibration), the higher recharge rates on St. George Island are of the order of magnitude of the $\sim$7 cm/year artificial R coming from aqueduct water. This suggests that the introduction of aqueduct water on St. George Island may be creating noticeable artificial R in some areas.

At some sites on St. George Island, however, human development (i.e., alteration of vegetation, surface cover, and elevation) may be reducing R, locally thinning the lens. This is seen most strongly in the central part of the model area (Fig. 11), where the inferred lens thickness requires negative R values reaching almost to the Gulf shore of the island. This is the most heavily developed area of the island (Fig. 3). Here there are large areas of asphalt (reducing infiltration), several large unlined retention ponds (increased ET), and very low dunes (increased ET). All of these factors have probably contributed to the loss of R in this area, resulting in a thinned lens locally deprived of R by human development.

These results indicate continued development on St. George Island will affect the freshwater lens in diverse ways. Increased consumption of aqueduct water may add additional R in developed areas, while erosion of dune topography on the Gulf side of the island should reduce R in that area. On the other hand, removal of the vegetation and infilling of the low-lying areas which are typical of the Bay side of the island could have the opposite effect. Recharge rates may increase, creating a thicker freshwater lens and a correspondingly larger flux of fresh groundwater to the Bay. For any of these scenarios, the calibrated groundwater models indicate that even local impacts (on scales of hundreds of meters) can perturb the form of the freshwater lens, and that these perturbations may persist year round.

Effect of near-shore water use on Dog Island

Dog Island has not experienced the same degree of development as St. George Island, and residents of the island rely solely on pumping of the freshwater lens for their water needs. In order to evaluate the effects of pumping fresh groundwater for household use on Dog Island, a 2-D model was constructed for the across-the-island transect shown in Fig. 10. Here the island is $\sim$600 m wide and the modeled maximum freshwater thickness is $\sim$16 m (slightly less than maximum thickness inferred from geophysical data, for reasons discussed above). This location was chosen because groundwater flow along this transect in the 3-D model was roughly perpendicular to the shores of the island, and can be approximated with a 2-D model. The model was discretized into 160, 5-m-wide columns, and 25, 1-m-thick layers. All aquifer parameters and recharge patterns are identical to those in the 3-D model on Dog Island (Fig. 10). After an initial model was obtained, two wells were inserted (in a 2-D model a well represents a linear sink continuous in the island parallel direction). These were located 100 m inland from the bay shore and 100 m inland from the Gulf shore (most houses on Dog Island are built within $\sim$100 m of the shore). The wells pump 1 gal/day (0.038 m^3/day) per meter of shore, from a depth of 3.5 m. This represents average household use of 50 gal/day (for a lot occupying 50 m of shoreline; occupation of homes on Dog Island is highly seasonal, this represents an annual average usage).

Figure 13 shows a plot of the initial location of the 1 and 10 kg/m^3 concentration contours, as well as their lo-

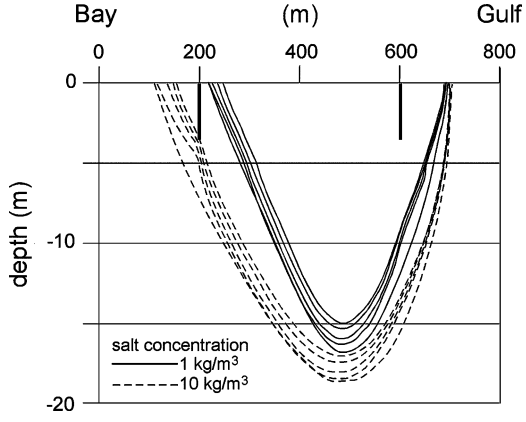

Fig. 13 Results of 2-D model representing impact of pumping on Dog Island freshwater lens. The configurations of the 1 and 10 kg/m^3 isochlors are shown for the initial model, then after 10, 20, 50 and 100 years of pumping (the lens shrinks with time)

 DOI 10.1007/s10040-005-0442-9

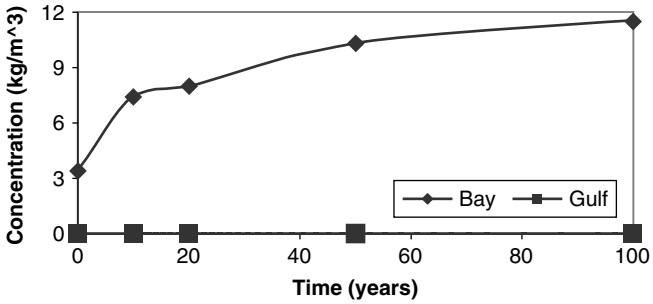

Fig. 14 Change in concentration over time in the Bay and Gulf wells for the Dog Island pumping model

cation after the model had run 10, 20, 50, and 100 years. Salt concentrations in the pumping wells at these times are displayed graphically in Fig. 14. The bay side well was initially pumping fairly salty water (~3 kg/m^3), and salt concentrations increased rapidly within the first 10 years (nearly 8 kg/m^3), and continued to gradually increase after that. At the surface, the 1 kg/m^3 boundary moved inland several tens of meters on the bay side. In contrast, the concentration contours on the Gulf side were only very slightly affected by pumping there. Initial salt concentration at this well was zero, and remained unchanged throughout the simulation. This is obviously due to the difference in recharge rates across the island, from up to 38 cm/year on the Gulf side to as little as −10 cm/year on the Bay side. As a result of pumping, the maximum lens thickness gradually thinned by ~2 m during the simulation, pulling the underlying mixing zone up as well. This modeling indicates that homes on the Bay side of Dog Island are at great risk of losing their fresh groundwater supply, where it exists, and that Bay side pumping may significantly increase salinity of groundwater discharged into the Bay. Low-density development on the Gulf side should not have a substantial impact on fresh groundwater availability and seaward groundwater discharge rates.

Impact of Island erosion on freshwater lens morphology

Regional 3-D models of these islands were not able to reproduce maximum freshwater lens thickness in some areas. Although model limitations, including the simple assumptions about K may be responsible, lens modification associated with island erosion offers another possible explanation. As previously discussed, Dog Island and St. George Island have experienced considerable erosion along both Gulf and Bay shores over the past 100 years. A 2-D model was constructed in order to test the theoretical impact of continuous island erosion on the freshwater and mixing zones. The initial calibrated model contained 200, 5-m-wide columns (1,000 m total) and 40, 1-m-thick layers. All aquifer parameters are identical to those in the 3-D models. The Gulf half of the island received a strongly positive R (38 cm/year) and the Bay side received a slightly negative R (−10 cm/year).

Erosion on Dog Island and St. George Island has averaged ~2 m/year on the Gulf shores and ~1 m/year on Bay shores for the past century (Schade 1986; Donoghue and Tanner 1994). The initial model was run to equilibrium with an island width of 800 m (outer 100 m on each side representing the Gulf and Bay). The model was then run over 5-year time spans, with the previous final heads and concentrations used as initial heads and concentrations. For each 5-year run, one cell (5 m) was taken from the island and added to the Bay and two cells (10 m) were taken from the island and added to the Gulf, matching the reported rates of erosion for these islands. After 100 years, the remaining island was 500 m wide. To compare the eroding island with a steady-state equivalent, the 500-m-wide island model was then run to steady-state as previously described for the 3-D models.

The resulting freshwater and mixing zones for the continuously eroded island and the 500-m-wide steady-state equivalent are shown in Fig. 15. The freshwater and mixing

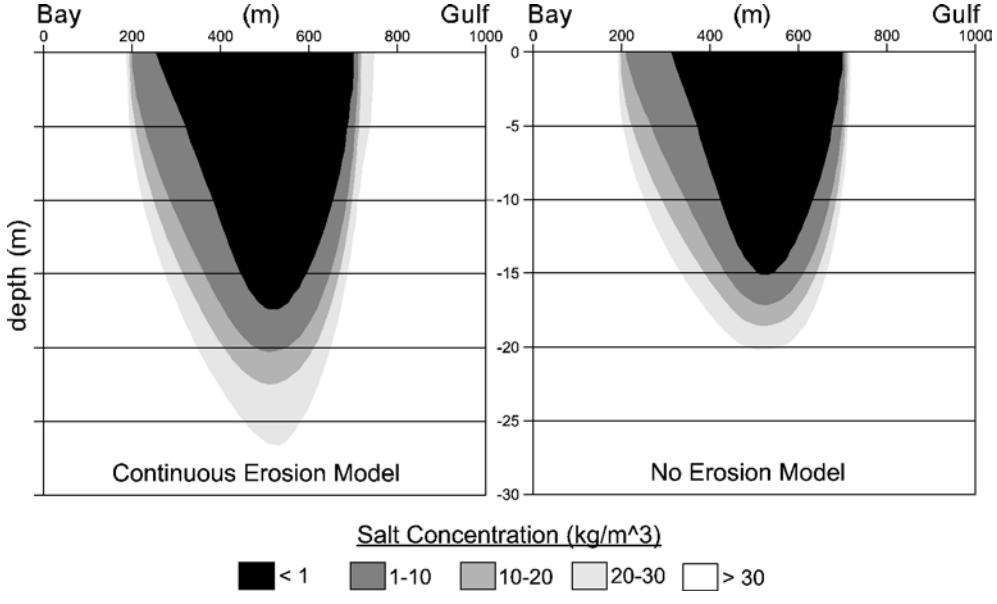

Fig. 15 Results of 2-D models assuming continuous erosion (2 m/year on Gulf shore and 1 m/year on Bay shore) and no erosion

DOI 10.1007/s10040-005-0442-9

zones for the island undergoing continuous erosion are larger than the steady-state island's freshwater and mixing zones; clearly the freshwater lens for the eroding island is not fully equilibrated to the new boundary conditions. The maximum fresh groundwater (i.e., <1 kg/m^3) thickness is $\sim$2 m greater, and the mixing zones extend several meters deeper for the continuously eroded island. This perhaps in part explains why the inferred maximum thickness of fresh groundwater is not reproduced in the models described in the previous section. These models also indicate that even if island erosion does not continue in the future, the lenses on these islands will thin as they approach equilibrium with current boundary conditions.

After erosion ceases in the eroded island model, progression toward equilibrium is more rapid at first and gradually slows, with a majority of the reduction in lens volume occurring during the first ten years. These results suggest that decadal-scale changes in boundary conditions (i.e., recharge, island shape) do significantly affect the total volume of these freshwater lenses.

Conclusions

Inferred patterns of fresh groundwater occurrence on Dog Island and St. George Island are more complicated than can be attributed to homogenous aquifer parameters and boundary conditions on these islands. Freshwater lens thickness is well correlated with the combined patterns of elevation and vegetation, and hence with R. Groundwater flow models were developed to test the hypothesis that variability in R may be the primary control on lens form. With three-dimensional, fully dispersive numerical models it was also possible to examine the potential impacts of selected natural and anthropogenic processes on such a lens. The following conclusions can be drawn.

1. Plausible spatial variability of R can account for the inferred lens asymmetry on St. George Island and Dog Island (though K variability may still be important locally).
2. Results of a model incorporating monthly variability expected in R agree with the observation that there is very little seasonal variability in the base of the freshwater lens on St. George Island. Though the surface of the freshwater lens does vary seasonally, this is apparently attenuated significantly within the aquifer (presumably due to the low hydraulic conductivity), so that seasonal variability in the base of the lens, if present, is insignificant.
3. On St. George Island, artificial R from aqueduct water may represent 7–25% of natural R. The recharge rates that achieve a satisfactory calibration of the St. George Island model are correspondingly higher than for many comparable terrains on Dog Island, possibly representing the artificial R from the aqueduct water.
4. Development on the central portion of St. George Island has locally thinned the lens. Observed and calibrated model hydraulic conductivities are sufficiently low that local perturbations persist.
5. The relatively sparse human population on Dog Island depends on the freshwater lens for their water needs. Groundwater modeling shows shallow groundwater extractions will have a much greater affect on the Bay side of the island, due to the much lower recharge rates there.
6. These islands have been continuously eroded over the past century; calibrated models indicate the freshwater lens is not in equilibrium with current boundary conditions; the lens will thin with time. This effect may account in part for the discrepancy between inferred and modeled steady-state maximum lens thickness.
7. The results discussed in (2) and (6) above indicate that the total volume of the freshwater lenses of these islands is relatively unaffected by short-term, intra-year variability in boundary conditions (i.e., recharge). It would appear that inter-year to decadal-scale variability (i.e., drought cycles, long-term climate change, gradual island migration) is required to significantly affect the total volume of the freshwater lenses of these islands.

Acknowledgments The study of Dog Island was funded by the Barrier Island Trust. St. George Island investigations were supported through a fellowship to J.C.S. from the NOAA National Estuarine Research Reserve program. We thank Lee Edmiston and the staff of the Apalachicola Bay Research Reserve, and Dianne Mellon of the Barrier Island Trust for logistical help and background material. Meghan Elliott, Nick Parker, Steve Scruggs, Darren Meadows, and Jim Inman contributed greatly to field work. We are grateful to Chris Langevin for making his SEAWAT code available and providing guidance with modeling. Mark Stewart, Peter Swarzenski, Tom Juster, Rick Oches, Chris Langevin, Perry Olcott, and an anonymous reviewer gave constructive reviews of the manuscript.

References

Anderson WP Jr, Evans DG, Snyder SW (2000) The effects of Holocene barrier-island evolution on water-table elevation, Hatteras Island, North Carolina, USA. Hydrogeol J 8:390–404

Ayers JF (1998) Groundwater flow dynamics beneath atoll islands. IAHS-AISH Publication 253:397–404

Collins WH III, Easley DH (1999) Fresh-water lens formation in an unconfined barrier-island aquifer. J Am Water Resour Assoc 35:1–21

Cooper HH (1959) A hypothesis concerning the dynamic balance of fresh water and salt water in a coastal aquifer. J Geophys Res 64:461–467

Corbett DR, Dillon K, Burnett W (2000) Tracing groundwater flow on a barrier island in the north-east Gulf of Mexico. Est Coast Shelf Sci

Davis RA (1994) Geology of Holocene Barrier Island Systems. Springer, Berlin Heidelberg New York

Davis RA (1997) The evolving coast. Scientific American Library, New York

Domenico PA, Schwartz FW (1998) Physical and chemical hydrogeology. Wiley, New York

Donoghue JF, Tanner WF (1994) Effects of near-term sedimentologic evolution on the lifetime of estuarine resources. NOAA Tech Memorand NOS SRD 27

Dunne T, Leopold LB (1978) Water in environmental planning. W.H. Freeman, New York

 DOI 10.1007/s10040-005-0442-9

Essaid HI (1990) The computer model SHARP, a quasi-three-dimensional finite-difference model to simulate freshwater and saltwater flow in layered coastal aquifer systems. USGS Water Resour Invest Rep, pp 90–4130

Ferris JG (1963) Cyclic water-level fluctuations as a basis for determining aquifer transmissibility. USGS Water-Supply Pap 1536-I:305–318

Fetter CW (1972) Position of the saline water interface beneath oceanic islands. Water Resour Res 8:1307–1315

Fetter CW (1993) Contaminant hydrogeology. Macmillan, New York

Guo W, Langevin CD (2002) User's guide to SEAWAT: acomputer program for simulation of three-dimensional variable-density ground-water flow. USGS Open-File Rep, pp 01–434

Harris WH (1967) Stratification of fresh and salt water on barrier islands as a result of differences in sediment permeability. Water Resour Res 3:89–97

Hubbert MK (1940) The theory of ground-water motion. J Geol 48:785–944

Kidd RE, Planert M (1985) Development of a fresh water supply from the water-table aquifer on a barrier island. Am Water Resour Assoc Tech Pub Series 85–1, pp 69–71

Langevin CD, Stewart MT, Beaudoin CM (1998) Effects of seawater canals on Fresh water resources: an example from Big Pine Key, Florida. Groundwater 36:503–513

Livingston RJ (1983) Resource atlas of the Apalachicola estuary. Florida Sea Grant College Report 55

Lloyd JW (1984) A review of some of the more important difficulties encountered in small island hydrogeological investigations. CSC Tech Publ Series 154:180–210

McDonald MG, Harbaugh AW (1988) A modular three-dimensional finite-difference ground-water flow model. USGS Survey Tech Water Resour Invest, p 6

Otvos EG (1985) Barrier island genesis—questions of alternatives for the Apalachicola coast, northeastern Gulf of Mexico. J Coastal Res 1:267–278

Ruppel C, Schultz G, Kruse S (2000) Anomalous freshwater lens morphology on a strip barrier island. Groundwater 38:872–881

Schade CJ (1986) Coastal processes, St. George Island, Florida. Suite statistics and sediment history. Proc Symp Coast Sedimentol 7:143–155

Schnable JE (1966) The evolution and development of part of the northwest Florida coast. PhD Thesis, Florida State University, Tallahassee, FL

Schneider JC, Kruse SE (2003) A comparison of controls on freshwater lens morphology of small carbonate and siliciclastic islands: examples form barrier islands in Florida, USA. J Hydrol 284:253–269

Simmons DL (1986) Geohydrology and ground-water quality on Shelter Island, Suffolk County, New York, 1983–84. USGS Water Resour Invest Rep 85-4165

Urish DW (1980) Asymmetric variation of a Ghyben-Herzberg lens. J Hydraulic Div, Proc, ASCE 107:1149–1158

Urish DW, Ozbilgin MM (1989) The coastal ground-water boundary. Groundwater 27:310–315

Vacher HL (1988a) Dupuit-Ghyben-Herzberg analysis of strip-island lenses. Geol Soc Am Bull 100:580–591

Vacher HL (1988b) Ground water in barrier islands—theoretical analysis and evaluation of the unequal-sea level problem. J Coastal Res 4:139–148

Vacher HL, Quinn T (eds) (1997) Geology and hydrogeology of carbonate islands. Elsevier, Amsterdam

Wallis TN, Vacher HL, Stewart MT (1991) Hydrogeology of freshwater lens beneath a Holocene strandplain, Great Exuma, Bahamas. J Hydrol 125:93–109

Wheatcraft SW, Buddemeier RW (1981). Atoll island hydrology. Groundwater 19:311–320

Whittecar GR, Johnson CJ (1990) Hydrogeologic analysis of water table fluctuations on a barrier island, Cape Henry, Virginia. Abstracts with programs. Geol Soc Am 22: 122–123

Whittecar GR, Johnson CJ (1991) Geologic and hydrologic controls of water tables on regressive barrier islands. Virginia J Sci 42: 222

Zheng C, Wang PP (1998) MT3DMS, A modular three-dimensional multispecies transport model for simulation of advection, dispersion and chemical reactions of contaminants in groundwater systems, Vicksburg, Miss., Waterways Experiment Station, US Army Corps of Engineers

 DOI 10.1007/s10040-005-0442-9